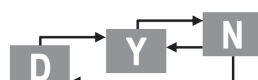


SCHRIFTENREIHE DES  
LEHRSTUHLS FÜR  
SYSTEMDYNAMIK UND PROZESSFÜHRUNG

Band 4/2024

Jesús David Hernández Ortiz

**Energy optimization of the steelmaking  
process in an electric arc furnace**



## **Energy optimization of the steelmaking process in an electric arc furnace**

Zur Erlangung des akademischen Grades eines  
**Dr.-Ing.**  
von der Fakultät Bio- und Chemieingenieurwesen der  
Technischen Universität Dortmund  
genehmigte Dissertation

vorgelegt von  
**M.Sc. Jesús David Hernández Ortiz**  
aus  
Bucaramanga, Kolumbien

Tag der mündlichen Prüfung: 27.09.2023

1. Gutachter: Prof. Dr. Sebastian Engell
2. Gutachter: Prof. Dr. Ian K. Craig

**Dortmund, 2023**



Schriftenreihe des Lehrstuhls für  
Systemdynamik und Prozessführung  
herausgegeben von Prof. Dr.-Ing. Sebastian Engell

Band 4/2024

**Jesús David Hernández Ortiz**

**Energy optimization of the steelmaking process  
in an electric arc furnace**

D 290 (Diss. Technische Universität Dortmund)

Shaker Verlag  
Düren 2024

**Bibliographic information published by the Deutsche Nationalbibliothek**

The Deutsche Nationalbibliothek lists this publication in the Deutsche Nationalbibliografie; detailed bibliographic data are available in the Internet at <http://dnb.d-nb.de>.

Zugl.: Dortmund, Technische Univ., Diss., 2023

Copyright Shaker Verlag 2024

All rights reserved. No part of this publication may be reproduced, stored in a retrieval system, or transmitted, in any form or by any means, electronic, mechanical, photocopying, recording or otherwise, without the prior permission of the publishers.

Printed in Germany.

ISBN 978-3-8440-9509-8

ISSN 1867-9498

Shaker Verlag GmbH • Am Langen Graben 15a • 52353 Düren

Phone: 0049/2421/99011-0 • Telefax: 0049/2421/99011-9

Internet: [www.shaker.de](http://www.shaker.de) • e-mail: [info@shaker.de](mailto:info@shaker.de)

# Abstract

Steel production via electric arc furnaces (EAFs) is a very energy-intensive process that accounts for almost 25% of the total crude steel production worldwide. In modern steelmaking, finding an economically beneficial mode of operation that reduces the energy consumption and the environmental impact of the process is the priority. In practice, however, achieving this goal is a challenging endeavor as the process is still not well understood and industrial operations rely strongly on the experience of the operating crews.

To address this challenge, this thesis presents a model-based optimization strategy that can reduce the energy demand of the EAF process. First, mathematical models of an electric arc and of an electric arc furnace were developed and used to answer two fundamental questions: a) How do the electrical setpoints of the furnace affect the geometry of the arc and the heat exchange between the arc and the metal phases in the furnace?, and b) How do various operative setpoints affect the melting dynamics of the process?. The developed models were validated using experimental and process data of an industrial ultra-high-power EAF.

Second, a dynamic optimization framework (DO) with the goal to minimize the electrical losses of the process is proposed. Two important operational questions were addressed: a) What is the optimal operation strategy that reduces the energy demand of the process?, and b) How can dynamic optimization and scheduling be integrated to achieve an optimal operation of the steelmaking plant?. The DO problem is solved using a control vector parametrization strategy that computes an optimal input trajectory for a batch of steel that consists of several charges. The computed control policy was tested in an industrial EAF, and the energy consumption of the process was reduced by 4.5% for a family of steels.

## Kurzfassung

Die Stahlerzeugung durch Elektrolichtbogenöfen (EAFs) ist ein sehr energieintensiver Prozess, der fast 25% der gesamten Rohstahlproduktion weltweit ausmacht. In der modernen Stahlerzeugung steht die Suche nach einer wirtschaftlich günstigen Betriebsweise im Vordergrund, die den Energieverbrauch der Anlage und die Umweltauswirkungen des Prozesses reduziert. In der Praxis ist das Erreichen dieses Ziels jedoch ein herausforderndes Unterfangen, da der Prozess immer noch nicht vollständig durchdrungen ist und der Betrieb in den Stahlwerken stark durch die Erfahrung der Anlagenfahrer bestimmt ist.

Um diese Herausforderung zu bewältigen, stellt diese Arbeit eine modellbasierte Optimierungsstrategie vor, die den Energiebedarf des EAF-Prozesses reduzieren kann. Zunächst wurden ein Lichtbogen-Modell und ein vollständiges EAF-Modell entwickelt. Die Modelle wurden verwendet, um vier grundlegende Fragen zu beantworten: a) Wie wirken sich die elektrischen Sollwerte des Ofens auf die Geometrie des Lichtbogens und den Wärmeaustausch aus?; b) Wie wirken sich verschiedene operative Sollwerte auf die Schmelzdynamik des Prozesses aus?; c) Was ist die optimale Betriebsstrategie, die den Energiebedarf des Prozesses reduziert?; und d) Wie können dynamische Optimierung und Planung integriert werden, um einen optimalen Betrieb zu erreichen? Die entwickelten Modelle wurden anhand von Versuchs- und Prozessdaten eines industriellen Ultrahochleistungs-EAF validiert.

Weiter wird ein dynamischer Optimierungsansatz mit dem Ziel, die elektrischen Verluste des Prozesses zu minimieren, vorgeschlagen. Die Lösung basiert auf der Steuerungsvektor-Parametrisierungsstrategie, und berechnet eine optimale Fahrweise für eine Reihe von Chargen, die in dem Ofen hintereinander bearbeitet werden. Die berechnete Fahrstrategie wurde in einem industriellen EAF getestet und der Energieverbrauch des Prozesses wurde für eine Gruppe von Stählen um 4,5% reduziert.

## Acknowledgments

First, I would like to express my gratitude to my supervisor Prof. Dr-Ing. Sebastian Engell for his guidance, input, commitment, and support.

I am also very grateful to the management team of the meltshop at Acciai Speciali Terni for having facilitated my work at the plant and for having allowed me to test in the production EAF the results of this thesis. I would like to specially thank Dr. Luca Onofri for his support and confidence in my work, to Mauro Grifoni and Lucio Mancini for all the shared knowledge in steelmaking, and to all the operators of the EAF that helped me during the validation tests.

Financial support is gratefully acknowledged from the Marie Skłodowska Curie Horizon 2020 EID-ITN project “PROcess NeTwork Optimization for efficient and sustainable operation of Europe’s process industries taking machinery condition and process performance into account – PRONTO”, Grant agreement No 675215.

# List of publications

The work carried out in this thesis led to the following publications:

## Journal articles

1. J. D. Hernández, L. Onofri, S. Engell, Numerical Estimation of the Geometry and Temperature of an Alternating Current Steelmaking Arc, *Steel. Res. Int.*, Vol. 92, 3, pp. 202000386(1-17), 2020.
2. T. Hay, J. D. Hernández, S. Roberts, T. Echterhof, Calculation of View Factors in Electric Arc Furnace Process Modeling, *Steel. Res. Int.*, Vol. 92, 2, pp. 202000341(1-14), 2020.
3. J. D. Hernández, L. Onofri, S. Engell, S., Modeling and energy efficiency analysis of the steelmaking process in an electric arc furnace, *Metall. Mater. Trans. B*, 53, pp. 3413–3441, 2022.

## Conference papers

4. J. D. Hernández, L. Onofri, S. Engell, Detailed modelling of radiative heat transfer in Electric Arc Furnaces using Monte Carlo techniques, in Proc. of the 8th Int. Conf. on Modeling and Simulation of Metallurgical Processes in Steelmaking (STEELSIM 2019), Toronto, Canada, pp. 295–306, 2019.
5. J. D. Hernández, L. Onofri, S. Engell, Model of an Electric Arc Furnace Oxy-Fuel Burner for dynamic simulations and optimization purposes, in Proc. of the 18th IFAC Symposium on Control, Optimization and Automation in Mining, Mineral and Metal Processing (IFACM2019), Stellenbosch, South Africa, Published in: *IFAC-PapersOnLine*, Vol. 52, 14, pp. 30-35, 2019.
6. J. D. Hernández, L. Onofri, S. Engell, Optimization of the electric efficiency of the electric steelmaking process, in Proc. of the 21st IFAC World Congress, Berlin, Germany, Published in: *IFAC-PapersOnLine*, Vol. 53, 2, pp. 11895-11900, 2020.
7. J. D. Hernández, L. Onofri, S. Engell, Energy optimization of the electric arc furnace for operations at a fixed electrical power level, in Proc. of the 19th IFAC Symposium on Control, Optimization and Automation in Mining, Mineral and Metal Processing (IFAC MMM2022), Montreal,

Canada, Published in: *IFAC-PapersOnLine*, Vol. 55, 21, pp. 144-149, 2022.

## **Book chapters**

8. J. D. Hernández, L. Onofri, S. Engell, Ch.4 Integrated modeling and energetic optimization of the steelmaking process in electric arc furnaces: An industrial application, in *Simulation and Optimization in Process Engineering. The Benefit of Mathematical Methods in Applications of the Chemical Industry*, Edited by: Michael Bortz and Norbert Asprion, pp. 77–100, Elsevier, 2022

## **Oral presentations**

9. J. D. Hernández, On the importance of the heat exchange modeling assumptions in electric arc furnace process models, in the 4th European academic symposium on EAF steelmaking, 16-18 June 2021, Aachen, Germany.
10. J. D. Hernández, L. Onofri, S. Engell, Energy optimization of the electric arc furnace for operations at a fixed electrical power level, in the 12th European electric steelmaking conference, 13–15 September 2021, Sheffield, UK.

## **Co-authored publications not part of this thesis**

11. G.C. Dalle Ave, J. D. Hernández, I. Harjunkoski, L. Onofri, S. Engell, Demand Side Management Scheduling Formulation for a Steel Plant Considering Electrode Degradation, in Proc. 12th IFAC Symposium on Dynamics and Control of Process Systems, including Biosystems DY-COPS 2019: Florianópolis, Brazil, Published in: *IFAC-PapersOnLine*, Vol. 52, 1, pp. 691-696, 2019.



# Contents

<b>List of Tables</b>	<b>XI</b>
<b>List of Figures</b>	<b>XIII</b>
<b>List of Symbols</b>	<b>XVII</b>
<b>1 Introduction</b>	<b>1</b>
1.1 Background and Motivation . . . . .	1
1.1.1 Steelmaking processes . . . . .	1
1.1.2 The electric arc furnace . . . . .	2
1.1.3 Steel types and their operational practices . . . . .	4
1.1.4 Setpoints and control structures . . . . .	6
1.1.5 Challenges in modern steelmaking . . . . .	7
1.1.6 Hierarchical structure for the optimization of the operation of the EAF steelmaking process . . . . .	9
1.2 Research objective and outline of the thesis . . . . .	12
1.2.1 General objective . . . . .	12
1.2.2 The knowledge gaps addressed by this thesis . . . . .	12
1.2.3 The industrial needs addressed by this thesis . . . . .	18
1.2.4 Thesis structure and outline . . . . .	19
<b>2 Modeling of steelmaking electric arcs</b>	<b>23</b>
2.1 What is an electric arc? . . . . .	23
2.2 State of the art in modeling of electric arcs . . . . .	24
2.2.1 Electric arc models using a first principles approach .	24
2.2.2 Channel arc models (CAM) . . . . .	27
2.2.3 Electric arc models from a purely electrical point of view	29
2.2.4 Arc models in steelmaking . . . . .	32
2.3 Derivation of a novel electric arc model for EAF . . . . .	34
2.3.1 Modeling approach and assumptions . . . . .	34
2.3.2 Governing equations . . . . .	35

2.3.3	Plasma parameters: electrical conductivity and Net Emission Coefficients . . . . .	41
2.3.4	The implicit NLP arc model . . . . .	42
2.4	Experimental measurements of the length of steelmaking arcs . . . . .	44
2.4.1	General descriptions . . . . .	44
2.4.2	Estimation of the depth of the slag layer . . . . .	45
2.4.3	Bath depression due to the jet of the arc . . . . .	45
2.4.4	Arc length measurements at a single electrical setpoint . . . . .	48
2.4.5	Arc length measurements at various electrical settings . . . . .	51
2.5	Determination of the free parameters of the model: arc radius and plasma composition . . . . .	54
2.6	Voltage and impedance effects on the physics of the arc . . . . .	60
2.6.1	Simplified approximation to the length of the arc . . . . .	62
2.6.2	Implicit approximation to the temperature of the arc . . . . .	64
2.7	Validation of the model and error estimations . . . . .	65
2.7.1	Estimation of the free parameters: empirical formula . . . . .	65
2.7.2	Estimation of the free parameters: Bowman's Formula . . . . .	66
2.7.3	Comparison of results and error computations of the predictions . . . . .	66
2.8	Summary of the chapter . . . . .	69
<b>3</b>	<b>Electric arc furnace process modeling</b> . . . . .	<b>71</b>
3.1	State of the art in EAF modeling . . . . .	71
3.2	Model development . . . . .	73
3.2.1	Causality between inputs and outputs . . . . .	73
3.2.2	Modeling assumptions . . . . .	73
3.2.3	Energy streams and energy balances . . . . .	78
3.2.4	Dynamic model . . . . .	80
3.2.5	Radiation from the arc . . . . .	82
3.2.6	Monte Carlo calculation of view factors . . . . .	89
3.2.7	Oxy-fuel burner model . . . . .	94
3.2.8	Oxidation of solid metals . . . . .	102
3.2.9	Combustion of coal . . . . .	103
3.2.10	Oxygen lancing . . . . .	104
3.3	Numerical results . . . . .	108
3.3.1	Melting rate and solid metal mass . . . . .	109
3.3.2	Temperature of the solid and the liquid metal phases . . . . .	111
3.4	Estimation of the free parameters of the model . . . . .	113
3.4.1	Formulation of the estimation problem . . . . .	113
3.4.2	Considered process data . . . . .	116
3.4.3	Results . . . . .	117

3.5	Validation of the model . . . . .	117
3.6	Summary of the chapter . . . . .	122
<b>4</b>	<b>Energy efficiency of the process</b>	<b>125</b>
4.1	Radiative energy flows and electrical energy efficiency . . . . .	125
4.2	Dynamic efficiency of the energy inputs . . . . .	128
4.3	Overall energy efficiency of the process . . . . .	129
<b>5</b>	<b>Model-based optimization of the EAF process</b>	<b>133</b>
5.1	Formulation of the optimal control problem for the electric energy efficiency of an EAF . . . . .	133
5.2	Strategies for the solution of the OCP . . . . .	135
5.3	Optimal operation at a single electrical power level . . . . .	136
5.3.1	Physics of the process and simplification of the OCP .	136
5.3.2	Effects of the geometry of the arc on the electrical energy losses of the process . . . . .	137
5.3.3	Optimal arc length for operations at a unique power level	141
5.4	Optimal operation using varying electrical power settings . .	143
5.4.1	Simplification and domain transformation of the OCP .	143
5.4.2	The control vector parametrization strategy . . . . .	145
5.4.3	Numerical case study and optimal mode of operation .	149
5.5	Results of the optimization in a real industrial process . . .	155
5.6	Outlook: Optimal plant-wide operation . . . . .	156
5.6.1	Reformulation of the OCP and integration with the scheduling layer . . . . .	156
5.6.2	Numerical case study of the integrated optimization .	157
5.7	Summary of the chapter . . . . .	159
<b>6</b>	<b>Summary and Conclusions</b>	<b>161</b>
<b>Bibliography</b>		<b>i</b>
<b>Appendix</b>		<b>xiii</b>



# List of Tables

2.1	Experimental results for the reference arc (451 V and 8.45 mΩ)	50
2.2	Experimental results for the different settings	52
2.3	Estimated arc temperatures and errors, NLP vs. result from (2.42)	64
2.4	RMSE for the empirical formula (Eq. 2.13) for standard values [87] and for estimated values of $V_{an\_ca}$ and $E_{arc}$	65
2.5	RMSE for the various cases of the Bowman Formula	66
2.6	Predictions of the different arc length computation methods	67
3.1	States of the switches in the DC circuit during the stages (a) to (b)	87
3.2	Results of the Monte Carlo algorithm for non blocking exchanges	91
3.3	Free parameters of the model	109
3.4	Parameters estimation table.	116
5.1	Total energy losses for different arc lengths and arc radii	139
5.2	Normalized values of the voltage, impedance and arc length inputs to the simulation timeline [V/V], [mΩ/mΩ], [cm/cm].	150
6.1	Summary of outcomes and contributions to the state of the art	164
A1	Electrical conductivity of air, iron and carbon plasmas $\sigma(T)$	xiii
A2	Net Emission Coefficient (NEC) of iron and carbon-air plasmas $\epsilon_N(T)$	xiv
A3	Resistors in the radiative circuit	xv
A4	Resistors in the radiative circuit	xvi
A5	Assumed surface temperatures and emissivities	xvii
A6	List of heat capacities	xvii



# List of Figures

1.1	An electric arc furnace . . . . .	3
1.2	Control structure for the electrical input . . . . .	6
1.3	Energy demand and, CO <sub>2</sub> emissions of the three most energy intensive industrial sectors . . . . .	7
1.4	EAF costs . . . . .	8
1.5	Functional hierarchy for batch processes* . . . . .	9
1.6	Proposed functional hierarchy for the EAF batch process . . . . .	11
1.7	Dynamic burner efficiency, Bergman approximation . . . . .	15
1.8	Optimization approach . . . . .	18
2.1	High voltage equivalent circuit of the EAF . . . . .	29
2.2	Wave forms for the square wave arc voltage model* . . . . .	30
2.3	Wave forms for the Cassie-Mayr model for various values of $\alpha^*$ . . . . .	31
2.4	Linear impedance model of an AC electric arc . . . . .	32
2.5	Radiative/Conductive properties of plasmas P1, P2 and P3 . . . . .	38
2.6	Assumed cavity geometries for different slag depths . . . . .	45
2.7	$\Psi$ , $d_c$ , $n_o$ vs. half-cone angle (sweep angle) . . . . .	47
2.8	Experimental procedure to measure the arc length . . . . .	49
2.9	Results of the Experiments 4 to 7 . . . . .	53
2.10	Parametric study of the solution point of the NLP in terms of $r_{a_{min}}$ and $\cos\phi = 0.8$ . . . . .	55
2.11	Solution space of the NLP . . . . .	57
2.12	RMSE at various values of $r_{a_{min}}$ . . . . .	58
2.13	Plasma temperatures for the 5 experimental arcs at the optimal $r_{a_{min}}$ values for the three plasma compositions . . . . .	59
2.14	Operative domain of the arc in an UHP-EAF . . . . .	60
2.15	Predicted influence of the voltage and impedance set-points on the length of the arc . . . . .	61
2.16	NLP surface, linear formula plane and experimental measurements . . . . .	63
2.17	Numerical vs experimental results . . . . .	68
2.18	Errors in the predictions of the models according to Eq. (2.43)	69

3.1	Geometry of the model and considered surfaces . . . . .	75
3.2	Geometries of the modeled melting stages . . . . .	77
3.3	The energy flows within the EAF model . . . . .	78
3.4	DC circuit equivalent representation of the heat exchange between two gray surfaces . . . . .	83
3.5	Circuital analysis for the arc surface . . . . .	85
3.6	DC circuit analogy of the heat exchange . . . . .	86
3.7	Coordinate system for the location and direction of emission of a bundle in a disc . . . . .	91
3.8	Primitives A to E of the hollowed-cylinder geometry . . . . .	92
3.9	Monte Carlo algorithm for exchanges with blockages* . . . . .	95
3.10	Assumed processes and geometry for the oxy-fuel combustion gases . . . . .	96
3.11	Geometrical configurations for the computation of the convective heat exchange . . . . .	100
3.12	Evolution of the mass of solid scrap over time for different models	110
3.13	Evolution of the solid metal temperature . . . . .	112
3.14	Evolution of the liquid metal temperature . . . . .	113
3.15	Cost surfaces of the estimation problems . . . . .	118
3.16	Process data vs simulation results (Normalized) . . . . .	119
3.17	Boredown time of the electrodes (Normalized) . . . . .	120
3.18	Normalized final melt temperature . . . . .	121
4.1	Radiative power arriving at each participating surface . . . . .	126
4.2	EAF dynamic electrical efficiency and losses . . . . .	127
4.3	Efficiencies of the energy inputs . . . . .	128
4.4	Normalized energy flows and net energy efficiency of the process	130
5.1	Dynamic energy losses for different arc lengths and radii . . . . .	138
5.2	Energy losses vs. mass of solid metal for different arc lengths .	140
5.3	Energy losses vs. arc length . . . . .	142
5.4	Electric arc length vs. operative power level for various values of $Z_a$ . . . . .	144
5.5	Discontinuities that result from the evaluation of the terminal conditions at the one-minute grid of the simulator . . . . .	148
5.6	Normalized energy fluxes vs. normalized batch time for the profile shown in Table 5.2 . . . . .	151
5.7	Electrical efficiency and losses of the EAF process if operated according to the profile in Table 5.2 . . . . .	151
5.8	Computed optimal power input and arc length . . . . .	152
5.9	Normalized KPIs for the base and the optimal case . . . . .	154

5.10	Improvements for the real process. Steel grade A . . . . .	155
5.11	Improvements for the real process. Steel grade B . . . . .	156
5.12	Optimal control policies for two final temperature requirements	158



# List of Symbols

Symbol	Description
<b>Latin</b>	
$a_{\perp}$	Cross section area of the arc ( $m^2$ )
$c_{psm}$	Solid metal heat capacity ( $kJ \ kg^{-1}$ )
$c_{pmm}$	Molten metal heat capacity ( $kJ \ kg^{-1}$ )
$c_{p(Fe_2O_3)}$	Oxides heat capacity ( $kJ \ kg^{-1}$ )
$c_{p(Fe_{2ox})}$	Iron heat capacity ( $kJ \ kg^{-1}$ )
$c_{pO_2}$	Oxygen heat capacity ( $kJ \ kg^{-1}$ )
$c_{pCO_2}$	Carbon dioxide heat capacity ( $kJ \ kg^{-1}$ )
$d_c$	Diameter of the cavity created by the arc in the molten metal ( $m$ )
$d_{sl}$	Depth of the slag layer ( $cm$ )
$g$	Gravity ( $m \ s^{-2}$ )
$h$	Height of the hollowed cylinder ( $m$ )
$j$	Axial component of the current density in the arc ( $A \ m^{-2}$ )
$k_{msm,1,2,3}$	Estimated melting rate parameter for the charge number 1, 2 and 3 (-)
$k_p$	Experimental constant: rate of formation of solid iron oxides ( $g^2 cm^{-4} s^{-1}$ )
$k_{sm}$	Thermal conductivity of the solid metal ( $kW \ m^{-1} K^{-1}$ )
$l_a$	Length of the arc ( $m$ )
$l_{a,meas}$	Measured length in the experiments ( $cm$ )
$m_{sm}$	Mass of solid metal ( $kg$ )
$m_{mm}$	Mass of molten metal ( $kg$ )
$n_o$	Depth of the cavity created by the arc in the molten metal ( $cm$ )
$r_a$	Radius of the arc ( $m$ )

Symbol	Description
$r_k$	Radius of the cathode spot in the electrode ( $m$ )
$u(x)$	Standard uncertainty in $x$
$x_i$	Molar fraction of component $i$ in the plasma ( $mol_i \ mol_{plm}^{-1}$ )
$A_i$	Area of the surface i ( $m^2$ )
$A_s c$	Total area of the solid metal in contact with the gaseous atmosphere ( $m^2$ )
$E$	Axial component of the electric field in the arc ( $V \ m^{-1}$ )
$I$	Electrical current ( $A$ )
$I_{R,a}$	Current of the resistive component of the AC arc ( $A$ )
$J_i$	Radiosity of the surface i
$N_B$	Blowing number (-)
$R_a$	Resistive component of the AC arc ( $\Omega$ )
$R_{eff}$	Internal radius of the hollowed cylinder ( $m$ )
$R_{fur}$	Radius of the furnace ( $m$ )
$T_a$	Temperature of the arc ( $K$ )
$T_f$	Temperature of fusion of the metal ( $K$ )
$T_i$	Temperature of the surface i in the radiative analysis ( $K$ )
$T_{mm}$	Temperature of the molten metal ( $K$ )
$T_{sm}$	Temperature of the solid metal ( $K$ )
$V_a$	Voltage of the AC arc ( $V$ )
$V_{R,a}$	Voltage of the resistive component of the AC arc ( $V$ )
$VF_{i-j}$	View factor from the surface i to the surface j (-)
$Z$	Zeta score (-)
$Z_a$	Impedance of the AC arc ( $\Omega$ )

## Greek

$\alpha$	Convexity constant of the NEC computation (-)
$\gamma$	Plasma thickness parameter ( $W \ sr^{-1} \ m^{-3} \ S^{-1}$ )
$\varepsilon_i$	Surface emissivity of the surface i (-)
$\epsilon_N$	Net Emission Coefficient NEC ( $W \ sr^{-1} \ m^{-3}$ )
$\eta_{LO_2}$	Efficiency of the oxygen lancing (-)
$\eta_x$	Efficiency of mechanism of heat exchange x (-)
$\mu_o$	Vacuum permeability ( $m \ kg \ s^{-2} \ m^{-2}$ )
$\Psi$	A-dimensional diameter over depth parameter of the arc (-)
$\rho_{sl}$	Density of the slag ( $kg \ m^{-3}$ )

Symbol	Description
$\rho_{mm}$	Density of the molten metal ( $kg\ m^{-3}$ )
$\rho_{sm}$	Density of the solid metal ( $kg\ m^{-3}$ )
$\sigma_b$	Stefan-Boltzmann constant ( $W\ m^{-2}\ K^{-4}$ )
$\sigma(T)$	Electrical conductivity of the plasma ( $S$ )
$\zeta_{sm}$	Fraction of splashed liquid metal that lands on the solid metal (-)
$\zeta_{mm}$	Fraction of splashed liquid metal that lands in the molten metal (-)
$\zeta_{w/r}$	Fraction of splashed liquid metal that lands on the roof and walls (-)

### Energy constants

$\Delta H_{(Fe_2O_3)}$	Enthalpy of formation of iron (III) oxide at 25 Deg C. ( $kJ$ )
$\Delta H_f$	Enthalpy of fusion of the solid metal ( $kJ$ )
$\Delta H_{L_{O_2M}}$	Enthalpy of reaction from the oxidation of metals in the liquid phase, due to lanced oxygen ( $kJ$ )
$\Delta H_{L_{O_2C}}$	Enthalpy of reaction from the oxidation of carbon in the liquid phase due to lanced oxygen ( $kJ$ )
$LHV_x$	Low Heating Value of the fuel x ( $kJ\ kg^{-1}$ )

### Flows of mater

$\dot{m}_{(Fe_{2ox})}$	Rate of generation of oxides in the solid metal ( $kg\ s^{-1}$ )
$\dot{m}_{(O_{2ox})}$	Mass flow rate of oxygen available for the oxidation of solid metal from the burners ( $kg\ s^{-1}$ )
$\dot{R}_B$	Total mass of splashed liquid metal due to the oxygen lancing ( $kg\ s^{-1}$ )
$\dot{F}_{O_2}$	Oxygen flow rate during lancing ( $m^3\ s^{-1}$ )
$\Delta M$	Mass of oxidized material ( $kg$ )

### Flows of energy

$\dot{Q}_{arc\_rad_{mm}}$	Energy flow from the arc to the molten metal ( $kW$ )
$\dot{Q}_{arc\_rad_{sm}}$	Energy flow from the arc to the solid metal for melting purposes ( $kW$ )
$\dot{Q}_{bur\_cond}$	Energy flow from the burner, convective contribution ( $kW$ )

Symbol	Description
$\dot{Q}_{bur\_rad}$	Energy flow from the burner, radiative contribution (kW)
$\dot{Q}_{coal}$	Energy flow released by the combustion of coal (kW)
$\dot{Q}_{loss}$	Energy flow from the bottom of the EAF to the environment (kW)
$\dot{Q}_{L_{O_2}}$	Net energy flow released by the oxidation of liquid metals and carbon dissolved in the bath due to oxygen lancing (kW)
$\dot{Q}_{L_M}$	Energy flow due to the oxidation of liquid metal in the liquid phase (kW)
$\dot{Q}_{L_C}$	Energy flow due to the oxidation of carbon in the liquid phase (kW)
$\dot{Q}_{L_{CO_2}}$	Energy flow to heating up the CO <sub>2</sub> gases generated in the bath to the temperature of the molten metal (kW)
$\dot{Q}_{mm\_cond_{sm\_h}}$	Energy flow from the molten metal to the bulk of solid metal via conduction mechanisms (kW)
$\dot{Q}_{net\_sm_m}$	Total energy flow for melting purposes (kW)
$\dot{Q}_{net\_sm_h}$	Total energy flow for heating of the solid metal (kW)
$\dot{Q}_{net\_mm_h}$	Total energy flow for heating of the liquid metal (kW)
$\dot{Q}_{ox_{sm}}$	Energy flow released by the oxidation of solid metals (kW)
$\dot{Q}_{smm\_cond_{sm\_h}}$	Energy flow from the solid metal in melting state to the bulk of solid metal via conduction mechanisms (kW)
$\dot{Q}_{sp_{sm}}$	Energy flow from the bath to the solid metal due to splashing (kW)
$\dot{Q}_{sp_{w/r}}$	Energy flow from the bath to the roof and the walls due to splashing (kW)

### Other symbols

$\cos\phi$	Power factor of the AC arc (-)
$\vec{E}$	Vectorial electric field ( $V m^{-1}$ )
$\vec{j}$	Vectorial current density ( $A m^{-2}$ )

---

<b>Symbol</b>	<b>Description</b>
<b>Abbreviations</b>	
AC	Alternating electrical current
AOD	Argon oxygen decarburization converter
APC	Advanced process control
BF	Blast furnace
BOF	Blowing oxygen furnace
CAM	Chanel arc model
CFD	Computational fluid dynamics
CVP	Control vector parametrization
DAE	Differential algebraic equation
DC	Direct electrical current
DO	Dynamic optimization
EAF	Electric arc furnace
KPI	Key performance indicator
MHD	Magneto-hydro-dynamic
MINLP	Mixed integer non-linear programming
NEC	Net emission coefficient
NLP	Non-linear programming
OCP	Optimal control problem
ODE	Ordinary differential equation
RMSE	Root mean squared error
UHP	Ultra high power

---